Magnetic and Kinetic Energy Spectrum of Whistler Turbulence: Particle-In-Cell Simulation

Shinji Saito*

Solar-Terrestrial Environment Laboratory,

Nagoya University, Nagoya 464-8601, Japan

S. Peter Gary†

Los Alamos National Laboratory, Los Alamos New Mexico 87545, USA

Yasuhito Narita‡

Institut für Geophysik und extraterrestrische Physik,

Technische Universität Braunschweig,

Mendelssohnstr. 3, D-38106 Braunschweig, Germany

(Dated: June 10, 2010)

Abstract

Whistler turbulence cascade is studied to understand essential properties of the energy spectrum at electron scales, by using a two-dimensional electromagnetic particle-in-cell (PIC) simulation. The simulation shows that the magnetic energy spectrum of forward-cascaded whistler turbulence exhibits a steeper power-law spectrum around $|k_\perp \lambda_e| \sim 1$ than that predicted by EMHD simulations and theories at relatively long wavelength, where $k_\perp$ is the wavenumber perpendicular to the mean magnetic field, and λ_e is the electron inertial length. A comparison of the spectral index from the PIC simulation with that predicted by the scaling law for short scales, suggests that the energy cascade at short scales includes the effect of not only magnetic fluctuations but also electron velocity fluctuations. The steep magnetic spectrum may support recent solar wind observations at the electron scales.

Introduction: The solar wind serves as a natural laboratory of collisionless plasma turbulence. Recent *in-situ* observations using the Cluster spacecraft[1, 2] showed the magnetic energy spectrum in solar wind turbulence at 1 AU over a frequency range from less than 10^{-2} Hz up to 10^{2} Hz. This frequency range covers scales from magnetohydrodynamics (MHD) to electron kinetic dynamics. These observations found two distinct breakpoints in the magnetic spectrum around the proton and electron inertial lengths.

At relatively low frequencies and long wavelengths, the inertial range solar wind turbulence is observed to have a frequency power-law index of about $-5/3$, reminiscent of the Kolmogorov inertial range spectrum for hydrodynamic turbulence. The first spectral breakpoint is observed at approximately 0.5 Hz, corresponding to $|k\lambda_p| \sim 1$, where k and λ_p are the wavenumber and the proton inertial length, respectively. This is followed at higher frequencies by a second regime with a steeper power-law dependence on frequency [3]. Near 20 Hz, a second spectral breakpoint is measured [1, 2]; this corresponds approximately to $|k\lambda_e| \sim 1$, where λ_e is the electron inertial length. At still higher frequencies a third regime is observed with still steeper frequency dependence [1, 2].

References [1, 4, 5] attributed their observations of the second regime to the cascade of kinetic Alfvén waves (KAWs) with Sahraoui *et al.* [1] giving the interpretation that these KAWs are dissipated beyond the second breakpoint. However, a theoretical study by Podesta *et al.* [6] suggests that the KAW cascade in the solar wind cannot reach electron scales because of its dissipation. They imply that the magnetic energy spectrum near the second breakpoint must be supported by fluctuations other than the KAW. Alexandrova *et al.* [2] argued that the steeper spectrum of the third regime is due to dissipation of fluctuations at electron scales.

Another plasma mode which may describe high-frequency turbulence observed in the solar wind is the whistler fluctuation. The electron-magnetohydrodynamics (EMHD) model can describe some aspects of whistler turbulence. The model assumes electrons as an incompressible fluid and protons as a stationary charge-neutralizing background. Biskamp *et al.* [7, 8] studied electron hydrodynamic turbulence in both two- and three-dimensional EMHD simulations, and showed that the magnetic energy spectrum is proportional to $k^{-7/3}$ and $k^{-5/3}$ at scales $|k\lambda_e| < 1$ and $|k\lambda_e| > 1$, respectively. Galtier and Bhattacharjee [9] used analytic theory and found an anisotropic power-law magnetic spectrum proportional to $k_{\perp}^{-5/2} k_{\parallel}^{-1/2}$, where the subscripts $\parallel$ and $\perp$ denote the directions parallel and perpendicular

to the mean magnetic field, respectively. Narita and Gary [10] also found a similar magnetic spectrum $E_B(k_\perp) \propto k_\perp^{-5/2}$ for both quasi-perpendicular and parallel interactions in their theory of whistler turbulence. These predictions are close to the spectral index observed at scales shorter than the proton inertial length and Larmor radius in the solar wind (e.g. [1–3, 11]). However, at scales around the electron inertial length and Larmor radius, the spectrum becomes steeper than the theoretical predictions, as observed by Cluster spacecraft [1, 2]. This may indicate either the dissipative effect of fluctuations or the breakdown of the cold plasma dispersion equation used in the EMHD approximation.

Gary *et al.* [12] and Saito *et al.* [13] presented electromagnetic particle-in-cell (PIC) simulations to study the energy cascade of whistler turbulence at relatively small amplitudes. They showed that the magnetic energy spectrum is anisotropic in the same sense as predicted by the EMHD model [9, 14, 15] in which the fluctuation energy cascades preferentially perpendicular to the mean magnetic field. This anisotropy is similar to that shown in the EMHD simulations, however the energy spectrum in the PIC simulations becomes steeper than the EMHD predictions. Possible reasons for the discrepancy are relatively strong Landau damping at $|k_\perp \lambda_e| \sim 1$ under the condition $\beta = 0.1$, or a different energy cascade mechanism in the kinetic regime, or both.

In this letter, we study whistler turbulence cascading from $|k\lambda_e| \ll 1$ to $|k\lambda_e| \sim 1$, using a two-dimensional electromagnetic particle-in-cell (PIC) simulation under the very low beta condition $\beta_e = 0.01$. This condition essentially eliminates whistler damping at $|k_\perp \lambda_e| \sim 1$, so the PIC simulation in this limit may be compared directly against computations using EMHD, which also has no wave-particle dissipation.

Simulation model: The simulation code used here is the relativistic electromagnetic particle-in-cell code, which is modified from the TRIdimensional STANford code [16]. Our code calculates three-dimensional velocity space response of each proton and electron superparticles in two spatial dimensions. Hence, our simulation includes full kinetic properties of plasma, contrary to other simulation models such as MHD and EMHD simulations. The simulation box size is $L_\parallel = L_\perp = 102.4\lambda_e$, where the electron inertial length contains 10 spatial grid points. The periodic boundary conditions for both directions are imposed on particles and electromagnetic fields. The total number of proton and electron superparticle pairs is about 6.7×10^7. Other initial physical dimensionless parameters are mass ratio $m_p/m_e = 1836$, temperature ratio $T_p/T_e = 1$, electron $\beta_e = 0.01$, and thermal speed

$v_{e,th}/c = 0.1$ and $v_{p,th} = v_e(m_p/m_e)^{-1/2}$, where subscripts p and e mean proton and electron, respectively, and c is the light speed.

We impose 42 right-hand polarized whistler waves at the initial time t = 0 in a homogeneous plasma. These wavenumbers are $k_\parallel \lambda_e = \pm 0.0613$, ± 0.1227, and ± 0.184, and $k_\perp \lambda_e = 0$, ± 0.0613, ± 0.1227, and ± 0.184. Frequencies for the waves are derived from the linear dispersion relation in a homogeneous collisionless plasma with physical parameters shown above. The fluctuating magnetic field $\delta\mathbf{B}$, electric field $\delta\mathbf{E}$, and electric current density $\delta\mathbf{J}$ of each mode satisfy Faraday's and Ampére's equations, where the electric current density is carried only by electrons ($\delta\mathbf{J} = -qn_e\delta\mathbf{v}_e$ assuming protons are at rest due to their large inertia in this relatively high frequency regime). At t = 0, each wave has an equal fluctuating amplitude, while phases are chosen using a uniform random function. The initial total magnetic fluctuation energy relative to the mean magnetic field energy $\epsilon_B = \sum_{n=1}^{42} (|\delta\mathbf{B}_n|^2/B_0^2)$ is 0.1 where n is a number of each mode.

Simulation results: Figure 1 shows the temporal evolution of the two-dimensional magnetic energy spectrum. The magnetic fluctuations imposed at $t = 0$ yield a forward cascade which transports the fluctuation energy preferentially in the $k_\perp$ direction in wavenumber space. This is the anisotropic property of whistler turbulence, which is consistent with the EMHD simulations and theories. The figures further show that the magnetic spectrum becomes more anisotropic as time increases. We focus on the reduced one-dimensional energy spectra as a function of $k_\perp$ to study the power-law scaling of whistler turbulence.

Figure 2 shows the reduced (a) magnetic and (b) electron velocity fluctuation energy spectra defined as

$$E_B(k_\perp) \equiv \frac{|B(k_\perp)|^2}{B_0^2} = \sum_{|k_\parallel \lambda_e|<0.5} \frac{|B(k_\parallel, k_\perp)|^2}{B_0^2}. \tag{1}$$

$$E_v(k_\perp) \equiv \frac{m_e n_e |v_e(k_\perp)|^2}{B_0^2/\mu_0} = \sum_{|k_\parallel \lambda_e|<0.5} \frac{m_e n_e |v_e(k_\parallel, k_\perp)|^2}{B_0^2/\mu_0}. \tag{2}$$

These spectra are averaged in time from $|\Omega_e|t \sim 2500$ to 3500. Dotted lines in (a) and (b) indicate power-law lines of spectral indices -4 and -2 respectively. As seen in figure 2(a), the spectral slope of magnetic fluctuations has the index about -4 at $|k_\perp \lambda_e| \sim 1$. This magnetic spectrum is clearly steeper than theoretical predictions published by several authors [7–10, 14, 15]. The spectrum of electron velocity fluctuations plotted in figure 2(b) shows a flatter spectrum with spectral index about -2. This flatter spectrum originates from

the relationship between magnetic fluctuation B_λ and electron fluctuation $v_{e,\lambda}$ at scale λ. At the high frequencies considered here, only electrons can respond to magnetic field fluctuations because of the large mass ratio m_p/m_e, so that the electric current $\mathbf{J}$ =rot$\mathbf{B}/\mu_0$ consists of only electron fluctuations. This relationship leads to $qn_e v_{e,\lambda} = kB_\lambda$, where $k \sim \lambda^{-1}$, and therefore the velocity spectrum is intrinsically flatter than the magnetic spectrum. The ratio of magnetic and electron velocity fluctuation energy is given as

$$\frac{n_e m_e v_{e,\lambda}^2}{B_\lambda^2/\mu_0} = (k\lambda_e)^2 \tag{3}$$

The magnetic fluctuation energy is dominant at $|k\lambda_e| \ll 1$, however at $|k\lambda_e| > 1$, the electron velocity fluctuation energy becomes larger. Our simulation results satisfy this relationship as seen in figure 2.

Figure 3 shows the temporal variations of spectral indices for the magnetic (red) and electron velocity (blue) spectra around $|k_\perp \lambda_e| \sim 1$. The spectral indices of magnetic and electron velocity fluctuations are close to -4 and -2 respectively for a long time. This indicates that whistler turbulence attains a quasi-steady, asymptotic state such that the energy cascade rate is larger than the dissipation rate. If dissipation were steepening the $k_\perp$ spectrum, that spectrum must shrink in $k_\perp$ direction in time with decaying fluctuation energy, as shown in the $\beta_e = 0.1$ simulations of Saito *et al.*[13]. But the $\beta_e = 0.01$ simulation here, figures 1 and 3 show the $k_\perp$ spectrum does not clearly shrink, and does not steepen in time, indicating that dissipation is ineffective at $|k_\perp \lambda_e| \sim 1$. Therefore, we conclude that a magnetic spectrum steeper than EMHD predictions is an essential property of whistler turbulence in the electron kinetic regime. We discuss why the spectrum should be so steep in next section by using whistler turbulence theory.

Scaling laws at the electron scales: To derive the scaling laws at electron kinetic scales, we modify two assumptions in EMHD. First, we assume the dispersion relation predicted by linear theory $\omega \propto k + const.$ (e.g. Figure 6.7 of Gary (1993) [17]). Several EMHD theories assume a long wavelength regime, where the dispersion relation is $\omega \propto k^2$. This relation may not be applied at short scales. Second, the energy cascade rate is also modified. Previous theories assume the energy cascade rate $\epsilon \sim B_\lambda^2/\tau_{cas}$, where B_λ is the magnetic fluctuation at wavelength λ, and τ_{cas} is the energy transfer time, indicating that the magnetic field fluctuation controls the energy cascade rate. This is because, as seen in equation 3, the magnetic fluctuation energy is dominant at a relatively long wavelength. However at

$|k\lambda_e| \sim 1$, the electron kinetic energy cannot be ignored. Here, we consider wave-wave interactions of whistler fluctuations following the dispersion relation $\omega \propto k + const.$ as magnetic energy fluctuations control the energy cascade, and as electron velocity fluctuations do.

We refer to the EMHD theory for quasi-parallel interactions discussed in Narita and Gary (2010) [10]. The group velocity in the parallel direction is

$$v_{g,\parallel} = \frac{\partial \omega}{\partial k_\parallel} \propto \frac{k_\parallel}{k_\perp} \tag{4}$$

where $k = \sqrt{k_\parallel^2 + k_\perp^2}$ and $k_\perp \gg k_\parallel$ because of the anisotropic property of whistler turbulence. The interaction time for whistler wave packets at quasi-parallel propagation is

$$\tau_{w,\parallel} = \frac{\lambda_\parallel}{v_{g,\parallel}} \propto \frac{k_\perp}{k_\parallel^2} \tag{5}$$

where $\lambda_\parallel$ is proportional to $k_\parallel^{-1}$. The cascade time for weak, incoherent, and quasi-parallel interactions is defined as

$$\tau_{cas,\parallel} = \frac{\tau_{ed}^2}{\tau_{w,\parallel}} \propto \frac{\lambda^2}{v_{e,\lambda}^2}\frac{k_\parallel^2}{k_\perp} \propto \frac{k_\parallel^2}{k_\perp k^4 B_\lambda^2} \tag{6}$$

where the eddy turnover time is $\tau_{ed} = \lambda / v_{e,\lambda}$, and $v_{e,\lambda} \propto kB_\lambda$. We consider two energy cascade rates by the quasi-parallel interactions of whistler wave packets ϵ_B and ϵ_v that are controlled by the fluctuations of the magnetic field and the electron velocity, respectively,

$$\epsilon_B = \frac{B_\lambda^2}{\tau_{cas,\parallel}} \propto \frac{k_\perp k^4 B_\lambda^4}{k_\parallel^2} \tag{7}$$

$$\epsilon_v = \frac{v_{e,\lambda}^2}{\tau_{cas,\parallel}} \propto \frac{v_{e,\lambda}^2 k_\perp k^4 B_\lambda^2}{k_\parallel^2} \propto \frac{k_\perp k^6 B_\lambda^4}{k_\parallel^2} \tag{8}$$

In the stationary state, the energy cascade rate is constant, which gives the two magnetic energy spectrum for ϵ_B and ϵ_v.

$$E_{B,B} \propto k_\perp^{-1} B_\lambda^2 \propto \epsilon_B^{1/2} k_\perp^{-7/2} \tag{9}$$

$$E_{B,v} \propto k_\perp^{-1} B_\lambda^2 \propto \epsilon_v^{1/2} k_\perp^{-9/2} \tag{10}$$

where we assumed $k_\parallel$ is constant, and $k_\perp \gg k_\parallel$. As the magnetic fluctuation energy determines the energy cascade rate, the predicted magnetic spectrum shows $\propto k_\perp^{-7/2}$. On the other hand, as the energy cascade rate is controlled by electron velocity fluctuations, the

magnetic spectrum shows $\propto k_\perp^{-9/2}$. Our PIC simulation shows the magnetic spectral index is about -4 which is between the spectral indices of $E_{B,B}$ and $E_{B,v}$. The simulation result suggests that the electron velocity and the magnetic fluctuation both are associated with the formation of the magnetic energy spectrum at $|k\lambda_e| \sim 1$ where the dispersion relation follows $\omega \propto k + const.$

In the case of quasi-perpendicular interaction, the cascade time is given as

$$\tau_{cas,\perp} = \frac{\tau_{ed}^2}{\tau_{w,\perp}} \propto \frac{1}{k^3 B_\lambda^2} \tag{11}$$

where $\tau_{w,\perp} = (k_\perp v_{g,\perp})^{-1}$ and $v_{g,\perp} = \partial\omega/\partial k_\perp$ is constant with assumption $k_\perp \gg k_\parallel$. Because $\tau_{cas,\parallel}/\tau_{cas,\perp} \propto k_\parallel^2/k_\perp^2 \ll 1$, the energy cascade of quasi-parallel interactions can be dominant at the electron scales.

Conclusion: We have presented a full kinetic electromagnetic particle-in-cell simulation for freely decaying whistler turbulence under the condition $\beta = 0.01$ where whistler damping is negligible at $|k_\perp\lambda_e| \leq 1$. In this case the energy cascade rate is considerably larger than the dissipation rate of fluctuations.

Whistler turbulence exhibits the anisotropic energy cascade which provides more fluctuation energy at a given wavenumber perpendicular to $\mathbf{B}_0$ than parallel (Figure 1). The reduced energy spectra (Eq.1) exhibit power-law spectra with an index of about -4 for the magnetic field and about -2 for electron velocity fluctuations around $|k_\perp\lambda_e| \sim 1$. The spectral slope of the magnetic energy is steeper than that predicted in the EMHD approximation.

As observed by the Cluster spacecraft [1, 2], the magnetic energy spectrum becomes steeper at electron scales. Although dissipative kinetic Alfvén waves may explain the steeper magnetic energy spectrum, our PIC simulation shows that whistler turbulence can also explain the steeper spectrum at the electron kinetic scales. Our simulation used the low β condition to reduce the dissipation effect by Landau resonance, under which the energy cascade rate is larger than the damping in whistler turbulence. If the dissipation effects are negligible at the electron kinetic scales, whistler turbulence explains the observations of the steeper magnetic energy spectrum.

By comparing the results of the simulation with the scaling law, the steeper magnetic energy spectrum is controlled by both magnetic and electron velocity fluctuations at $|k\lambda_e| \sim 1$. But the EMHD simulations assuming the cold plasma dispersion relation do not show the steep magnetic spectrum even at $|k\lambda_e| \sim 1$ [7, 8]. This discrepancy between the EMHD

and the PIC simulation suggests that the energy cascade process includes electron kinetic effects at the short scales. Further theoretical and simulation studies should be required to understand physical processes for cascading the fluctuation energy with electron kinetic effects.

Acknowledgement: This work was supported by Grant-in-Aid for Young Scientists (B) 21740353 from Japan Society for the Promotion of Science.

The Los Alamos portion of this work was performed under the auspices of the U.S. Department of Energy (DOE). It was supported by the Solar and Heliospheric Physics SR&T and Heliophysics Guest Investigators Programs of the National Aeronautics and Space Administration.

FIGURE CAPTIONS

Figure 1: Temporal evolution of magnetic energy spectrum normalized by the mean magnetic field energy at $|\Omega_e|t = 0$, ~ 1000, ~ 2000, and ~ 3000, plotted by color and line contours. The value is shown as log-scale.

Figure 2: The reduced (a) magnetic and (b) electron velocity fluctuation energy spectra as a function of $k_\perp$, normalized by the mean magnetic field energy. Dotted lines shown in (a) and (b) are spectral slopes with power-law indices -4 and -2, respectively.

Figure 3: Time evolution of spectral indices of (red) magnetic and (blue) electron velocity fluctuation energy spectra fit over $0.6 \leq |k_\perp \lambda_e| \leq 3.0$.

---

* saito@stelab.nagoya-u.ac.jp

† pgary@lanl.gov

‡ y.narita@tu-bs.de

[1] F. Sahraoui, M. L. Goldstein, P. Robert, and Y. V. Khotyaintsev, Phys. Rev. Lett. **102** (2009).

[2] O. Alexandrova, J. Saur, C. Lacombe, A. Mangeney, J. Mitchell, S. J. Schwartz, and P. Robert, Phys. Rev. Lett. **103** (2009).

[3] C. W. Smith, B. J. Vasquez, and K. Hamilton, J. Geophys. Res. **111**, A09111 (2006).

[4] R. J. Leamon, C. W. Smith, N. F. Ness, and W. H. Matthaeus, J. Geophys. Res. **103**, 4775 (1998).

[5] S. D. Bale, P. J. Kellogg, F. S. Mozer, T. S. Horbury, and H. Reme, Phys. Rev. Lett. **94**, 215002 (2005).

[6] J. J. Podesta, J. E. Borovsky, and S. P. Gary, Astrophys. J. **712**, 685 (2010).

[7] D. Biskamp, E. Schwarz, and J. F. Drake, Phys. Rev. Lett. **76**, 1264 (1996).

[8] D. Biskamp, E. Schwarz, A. Zeiler, A. Celani, and J. F. Drake, Phys. Plasmas **6**, 751 (1999).

[9] S. Galtier and A. Bhattacharjee, Phys. Plasmas **10** (2003).

[10] Y. Narita and S. P. Gary, Ann. Geophys. **28**, 597 (2010).

[11] K. H. Kiyani, S. C. Chapman, Y. V. Khotyaintsev, M. W. Dunlop, and F. Sahraoui, Phys. Rev. Lett. **103** (2009).

[12] S. P. Gary, S. Saito, and H. Li, Geophys. Res. Lett. **35**, L02104 (2008).

[13] S. Saito, S. P. Gary, H. Li, and Y. Narita, Phys. Plasmas **15**, 102305 (2008).

[14] S. Dastgeer and G. P. Zank, Astrophys. J. **599**, 715 (2003).

[15] J. Cho and A. Lazarian, Astrophys. J. Lett. **615**, L41 (2004).

[16] O. Buneman, "Computer space plasma physics: Simulation techniques and software," (Terra Sci., 1993) Chap. 3, p. 67.

[17] S. P. Gary, *Theory of space plasma microinstabilities* (Cambridge University Press, 1993).

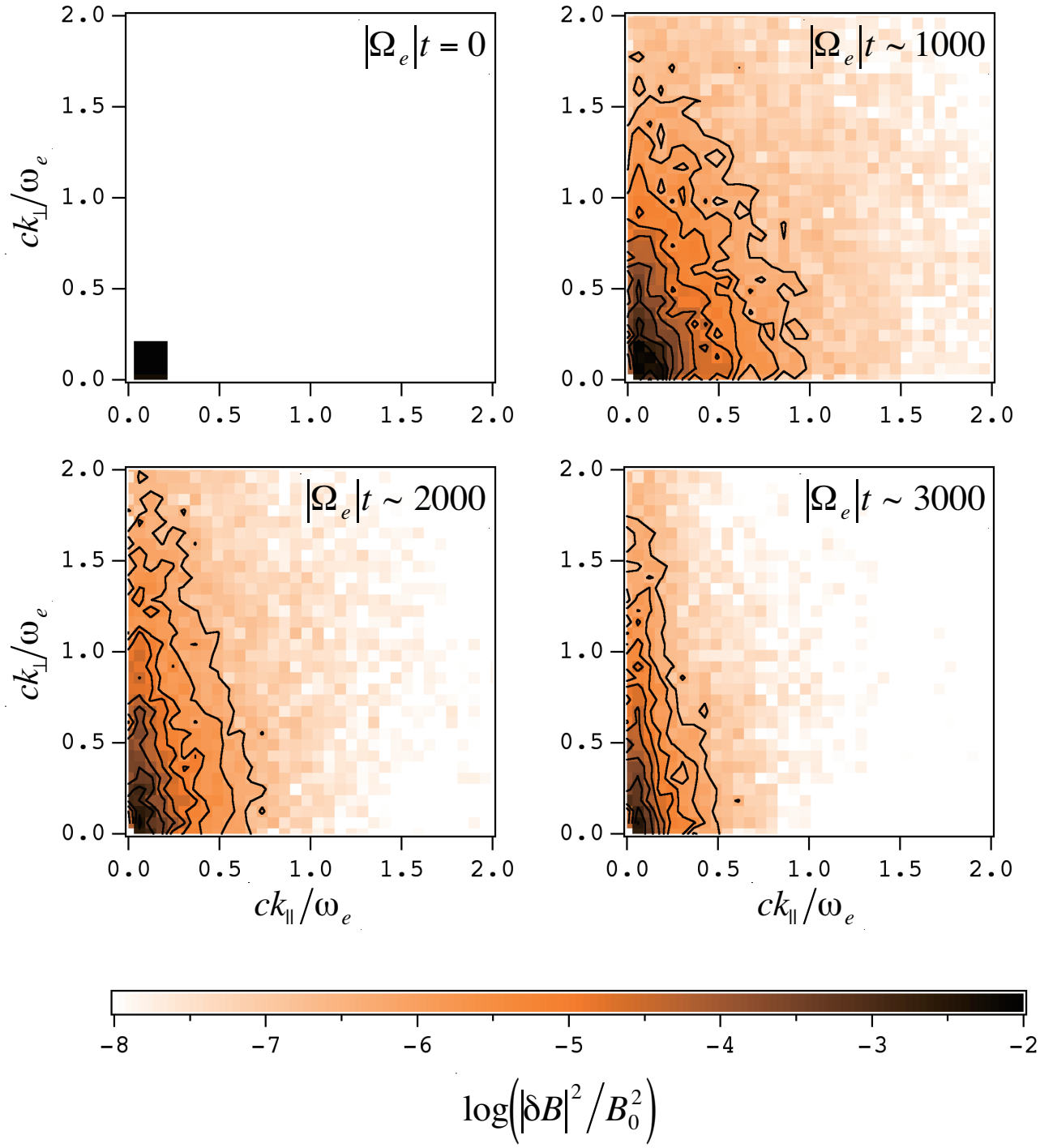

Figure 1 10Jun2010

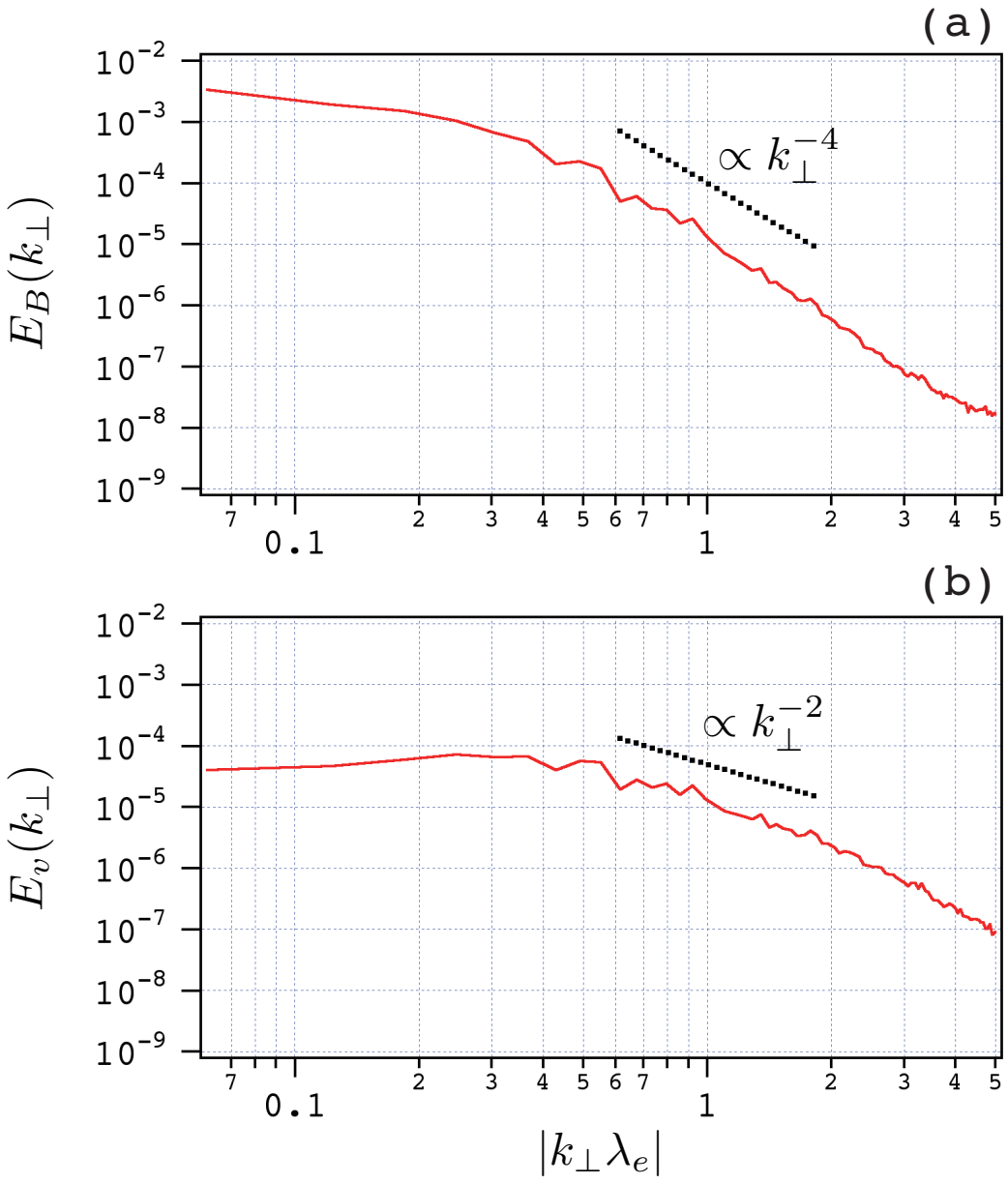

Figure 2 10Jun2010

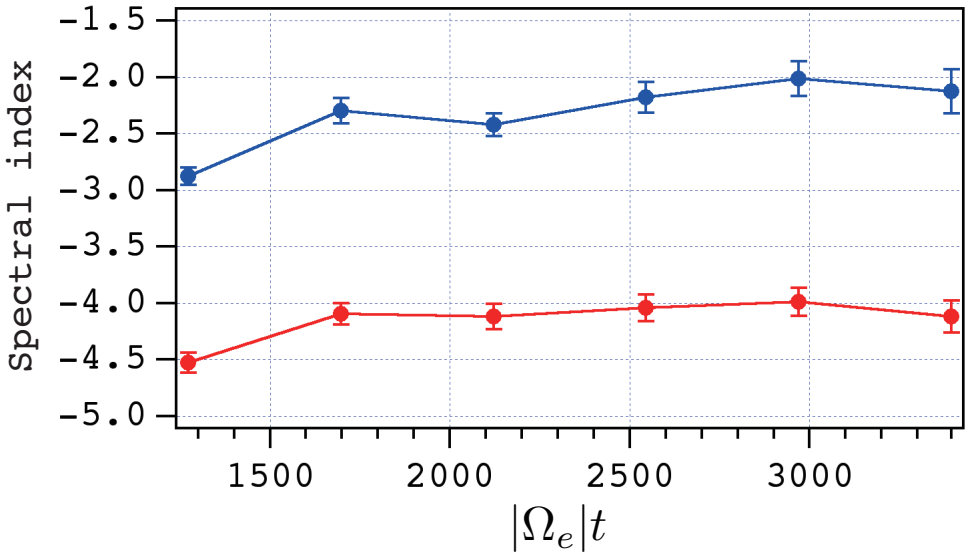

Figure 3 10Jun2010